



UNIVERSITY OF
ARKANSAS



Evidence that Spiral Arms in Disk Galaxies Are Produced by Density Waves

Benjamin L. Davis
University of Arkansas



Abstract

Spiral structure is the most distinctive feature of disk galaxies and yet debate persists about which theory of spiral structure is the correct one. The best known theory holds density waves propagating through the disk of the galaxy as the responsible agent, either via a standing wave pattern, or a more transient succession of waves crossing the disk. Other theories pose completely different agents, such as the manifold theory, which argues that the spiral arms arise because of stars moving in chaotic orbits. The standing (or modal) density wave theory demands that the pitch angle be uniquely determined by the distribution of mass in the bulge and disk of the galaxy. We present evidence that the tangent of the pitch angle of logarithmic spiral arms in disk galaxies correlates strongly with the density in neutral atomic hydrogen in the disk of the galaxy and with the central stellar bulge mass of the galaxy. These three quantities, when plotted against each other, form a planar relationship which, we argue, should be fundamental to our understanding of spiral structure in disk galaxies. We further argue that any successful theory of spiral structure must be able to explain this relationship. The low scatter in the relationship, if replicated in larger samples, may suggest that the standing wave picture is the correct one, at least for most disk galaxies.

Introduction

Spiral structure is a commonplace and visually obvious feature of many galaxies (which were at one time referred to as “spiral nebulae”) and yet there is still debate as to the correct theory which explains its origin. The density wave theory has been studied for several decades now and still has many supporters, divided broadly into two camps: those who contend that the spiral pattern is a long-lasting one created by standing waves (the modal theory) and others who regard the pattern as transient (compared to the lifetime of a galaxy), though perpetually recreated as new density wave patterns emerge (the swing amplification theory). Other theories have also been proposed, with one in particular, the Manifold theory, rejecting the density wave concept altogether, in favor of an explanation involving stars in chaotic highly eccentric orbits.

The density wave theory has had one outstanding success since its creation, not as applied to galaxies, but in the context of patterns observed in Saturn’s rings. In the limit of a very large central mass and a thin disk, the pitch angle of these density waves, as shown by Shu (1975), depends on the ratio of the disk mass density to the central mass. Specifically,

$$\tan|P| \propto \frac{\Sigma(R)}{M(R)}, \quad (1)$$

where P is the logarithmic spiral arm pitch angle, $\Sigma(R)$ is the disk surface density measured at a given radius of R , and $M(R)$ is the mass of the central planet. Galaxies are generally more complex than Saturn’s rings, for instance only very bulge-dominated galaxies are even close to the Saturn-like situation of a small dense core with negligible mass in the disk. Studies based on the modal density wave theory suggest that the pitch angle of the spiral arms in galaxies should still depend on a ratio (of half-mass radius to co-rotation radius) which, in limit of a thin disk and massive central bulge, approximates to the Shu (1975) result (Equation (1)). This is not surprising, since we would expect a standing wave pattern to depend on the ratio of a restoring force or tension (in this case the central mass, or at least the mass inside a given radius R) to the density of the medium (in this case the density of gas in the disk at radius R). Although the precise nature of the relation between these three quantities can be expected to vary between galaxies of different types (bulge-dominated versus disk-dominated, for instance) nevertheless we show in this letter that the three quantities, spiral arm pitch angle, central bulge mass, and gas density in the disk do strongly correlate to form a fundamental plane which may play a similar role in tying together gross features of disk galaxies to that played by the fundamental plane of elliptical galaxies (Djorgovski & Davis 1987; Dressler et al. 1987).

We studied a sample of disk galaxies from the Disk Mass Survey (DMS) which was ideal for our purposes, since it dealt with the disk densities of a sample of face-on galaxies. The DMS had already measured the gas density of atomic hydrogen in these galaxies, as well as the central bulge mass. Using our established technique (Davis et al. 2012) we measured the pitch angle for these galaxies for this paper. We find that the sample of 24 galaxies from the DMS, when plotted in a volume defined by these three quantities, delineate a plane which they stay close to with very low scatter. There is only a 0.002% chance that this plane could have been formed by statistical accident.

Results

TABLE 1 SAMPLE								
Galaxy Name (1)	Type (2)	Band (3)	Image Source (4)	m (5)	$\tan P $ (6)	$\log(M_*^{\text{bulge}}/M_\odot)$ (7)	$\Sigma_{H_I}^{\max}/(M_\odot pc^{-2})$ (8)	Excluded (9)
Milky Way	SBc	21 cm	1	4	0.41 ± 0.05^a	9.95 ± 0.03^b	$4.98 \pm 0.53^{c,d}$	
UGC 448	SABc	<i>r</i>	2	4	0.33 ± 0.03	$9.76^{+0.23}_{-0.21}$	4.58 ± 0.46	
UGC 463	SABc	<i>B</i>	3	3	$0.41^{+0.07}_{-0.06}$	$9.35^{+0.16}_{-0.15}$	6.18 ± 0.66	
UGC 1081	SBc	<i>r</i>	2	2	$0.45^{+0.07}_{-0.06}$	$8.81^{+0.16}_{-0.15}$	6.25 ± 0.62	
UGC 1087	Sc	<i>r</i>	2	2	0.19 ± 0.04	$8.64^{+0.16}_{-0.15}$	4.42 ± 0.46	
UGC 1529	Sc	645.0 nm ^e	4	3	$0.49^{+0.10}_{-0.09}$	$8.98^{+0.20}_{-0.19}$	6.59 ± 0.66	
UGC 1635	Sbc	<i>r</i>	2	3	0.21 ± 0.01	$8.74^{+0.17}_{-0.29}$	2.60 ± 0.32	
UGC 1862	SABed ^f	<i>r</i>	2	2	$0.44^{+0.08}_{-0.07}$...	9.14 ± 0.91	✓
UGC 1908	SBc ^g	645.0 nm ^e	4	3	0.38 ± 0.07	$9.68^{+0.23}_{-0.24}$	4.62 ± 0.46	
UGC 3091	SABd	<i>i</i>	2	2	$0.56^{+0.10}_{-0.09}$...	5.59 ± 0.56	✓
UGC 3140	Sc	<i>r</i>	2	3	0.29 ± 0.09	$9.65^{+0.15}_{-0.14}$	4.87 ± 0.54	
UGC 3701	Sed	<i>r</i>	2	2	0.28 ± 0.09	$8.69^{+0.18}_{-0.17}$	5.55 ± 0.57	
UGC 3997	Im	<i>g</i>	5	2	0.18 ± 0.05	$8.53^{+0.21}_{-0.20}$	5.01 ± 0.54	
UGC 4036	SABbc	645.0 nm ^e	4	2	0.27 ± 0.02	$8.92^{+0.15}_{-0.13}$	5.20 ± 0.56	
UGC 4107	Sc	<i>g</i>	5	2	0.37 ± 0.04	$8.65^{+0.18}_{-0.17}$	5.42 ± 0.54	
UGC 4256	SABc	<i>g</i>	5	2	0.56 ± 0.10	$9.29^{+0.26}_{-0.25}$	9.75 ± 0.98	
UGC 4368	Scd	<i>g</i>	5	2	0.44 ± 0.04	$9.21^{+0.21}_{-0.21}$	5.95 ± 0.66	
UGC 4380	Scd	<i>g</i>	5	3	$0.43^{+0.10}_{-0.09}$	$8.86^{+0.13}_{-0.13}$	4.08 ± 0.41	
UGC 4458	Sa	<i>g</i>	5	1	0.24 ± 0.06	$10.67^{+0.20}_{-0.20}$	3.28 ± 0.53	
UGC 4555	SABbc	<i>g</i>	5	2	0.21 ± 0.02	$8.96^{+0.19}_{-0.19}$	4.58 ± 0.47	
UGC 4622	Scd	<i>g</i>	5	4	0.40 ± 0.10	$9.89^{+0.21}_{-0.21}$	3.50 ± 0.38	
UGC 6903	Sbcd	<i>g</i>	5	2	0.28 ± 0.04	$8.02^{+0.21}_{-0.21}$	4.94 ± 0.59	
UGC 6918	SABb ^h	F606W	6	3	0.31 ± 0.04	$8.04^{+0.06}_{-0.04}$	7.04 ± 0.72	✓
UGC 7244	Sbcd	<i>g</i>	5	2	$0.63^{+0.11}_{-0.10}$...	5.53 ± 0.60	✓
UGC 7917	Sbbc	<i>g</i>	5	3	0.28 ± 0.03	$10.01^{+0.34}_{-0.31}$	2.70 ± 0.28	✓
UGC 8196	Sb	<i>g</i>	5	5	0.14 ± 0.01	$10.73^{+0.26}_{-0.26}$	2.74 ± 0.28	
UGC 9177	Scd	<i>g</i>	5	2	0.26 ± 0.03	$9.55^{+0.24}_{-0.24}$	3.92 ± 0.42	
UGC 9837	SABc	<i>g</i>	5	6	0.48 ± 0.06	$8.35^{+0.17}_{-0.17}$	7.95 ± 0.80	
UGC 9965	Sc	<i>g</i>	5	3	0.24 ± 0.04	...	5.63 ± 0.58	✓
UGC 11318	SBbc	645.0 nm ^e	4	3	$0.57^{+0.11}_{-0.10}$	$9.69^{+0.23}_{-0.20}$	6.51 ± 0.67	
UGC 12391	SABc	<i>r</i>	2	4	0.23 ± 0.09	$8.98^{+0.17}_{-0.28}$	4.90 ± 0.49	

NOTE.—Columns: (1) Galaxy name, (2) Hubble type from either the UGC (Nilson 1973) or RC3 (de Vaucouleurs et al. 1991) catalogs. Notes on morphologies: 1 = peculiar, 2 = starburst, and 3 = AGN. (3) Filter/waveband/wavelength used for pitch angle calculation. (4) Telescope/literature source of imaging used for pitch angle calculation. (5) Harmonic mode (number of spiral arms). (6) Tangent of the pitch angle of the galactic logarithmic spiral arms. (7) Base 10 logarithm of the stellar bulge mass of the galaxy, in solar masses. (8) Maximum surface density in the galactic H_I gas, in solar masses per square pc. (9) Indication of galaxies that are excluded in subsequent fittings due to missing measurements or measurements that are merely upper limits. *Image Sources:* (1) Levine et al. (2006); (2) WIYN 3.5 m pODI; (3) JKT 1.0 m; (4) Palomar 48 inch Schmidt; (5) SDSS; (6) HST.

^a Levine et al. (2006).

^b McMillan (2011).

^c No error estimates were provided by its reference so we have assigned the mean error of the included sample, $\pm 0.53 M_\odot pc^{-2}$.

^d Calculated using Equation 2 from Ferrière (2001).

^e IIIa emulsion.

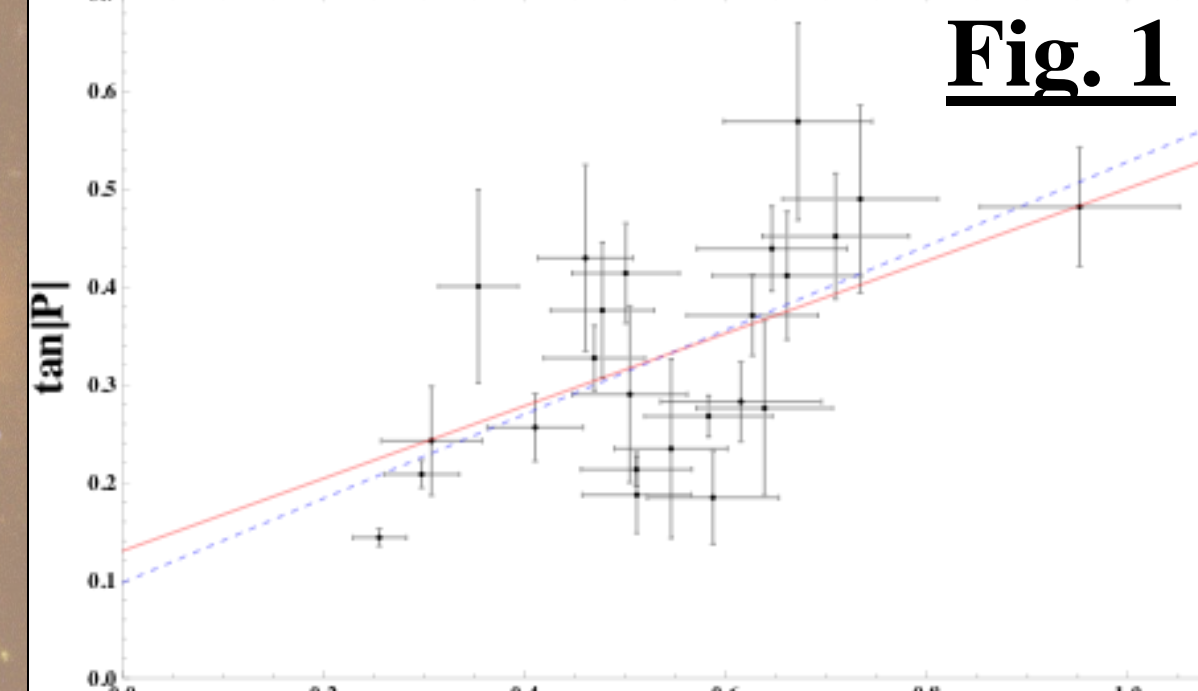


Fig. 1

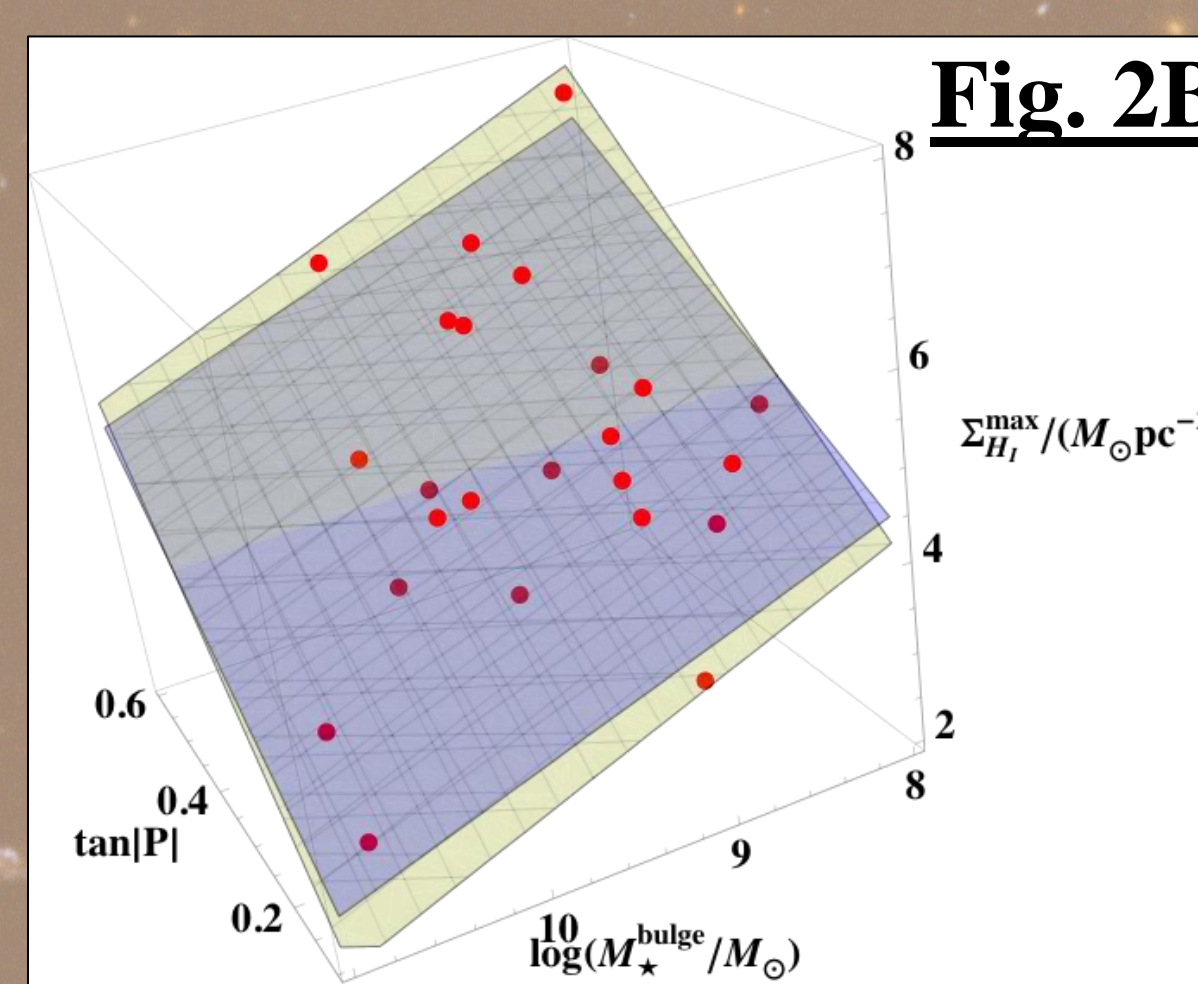


Fig. 2A

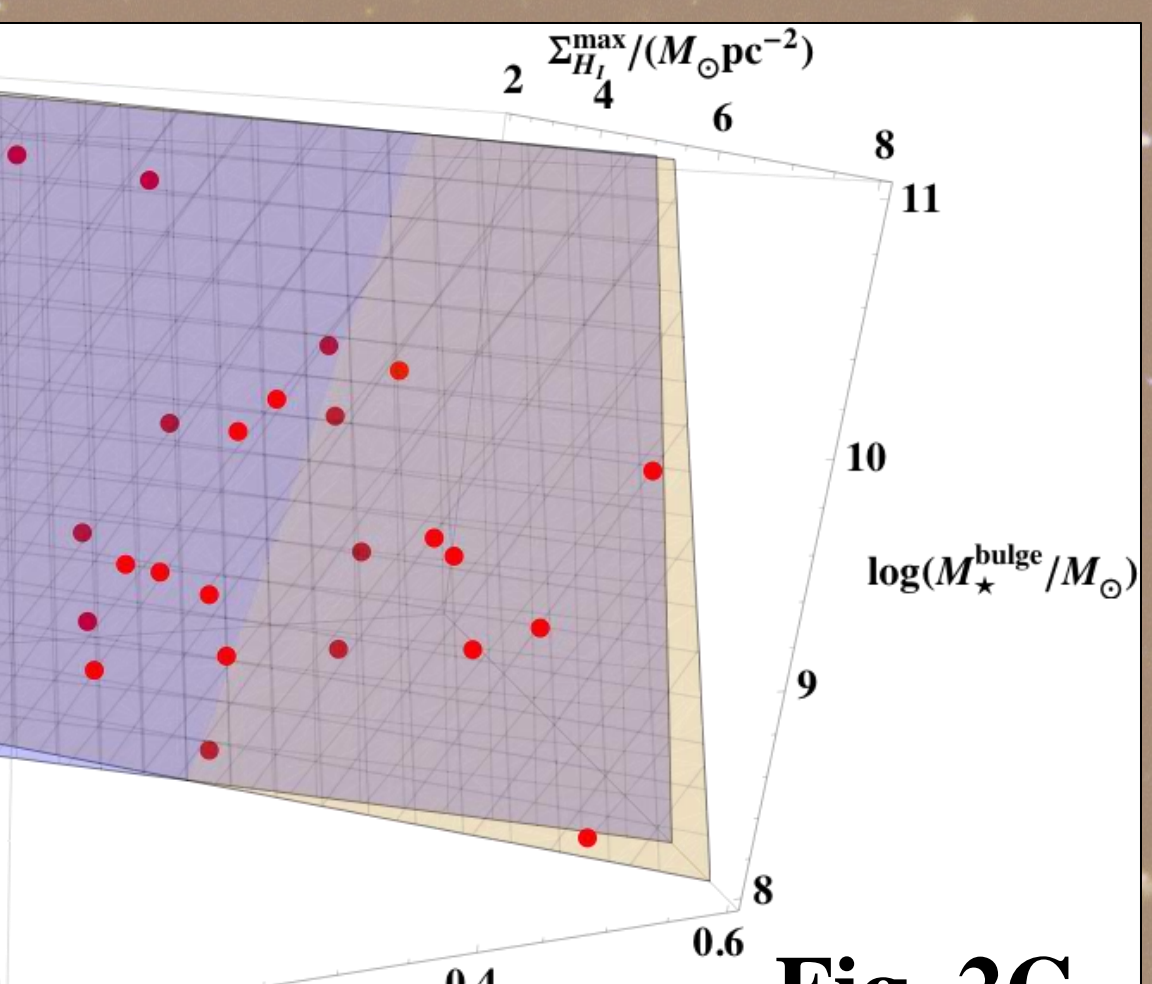


Fig. 2B

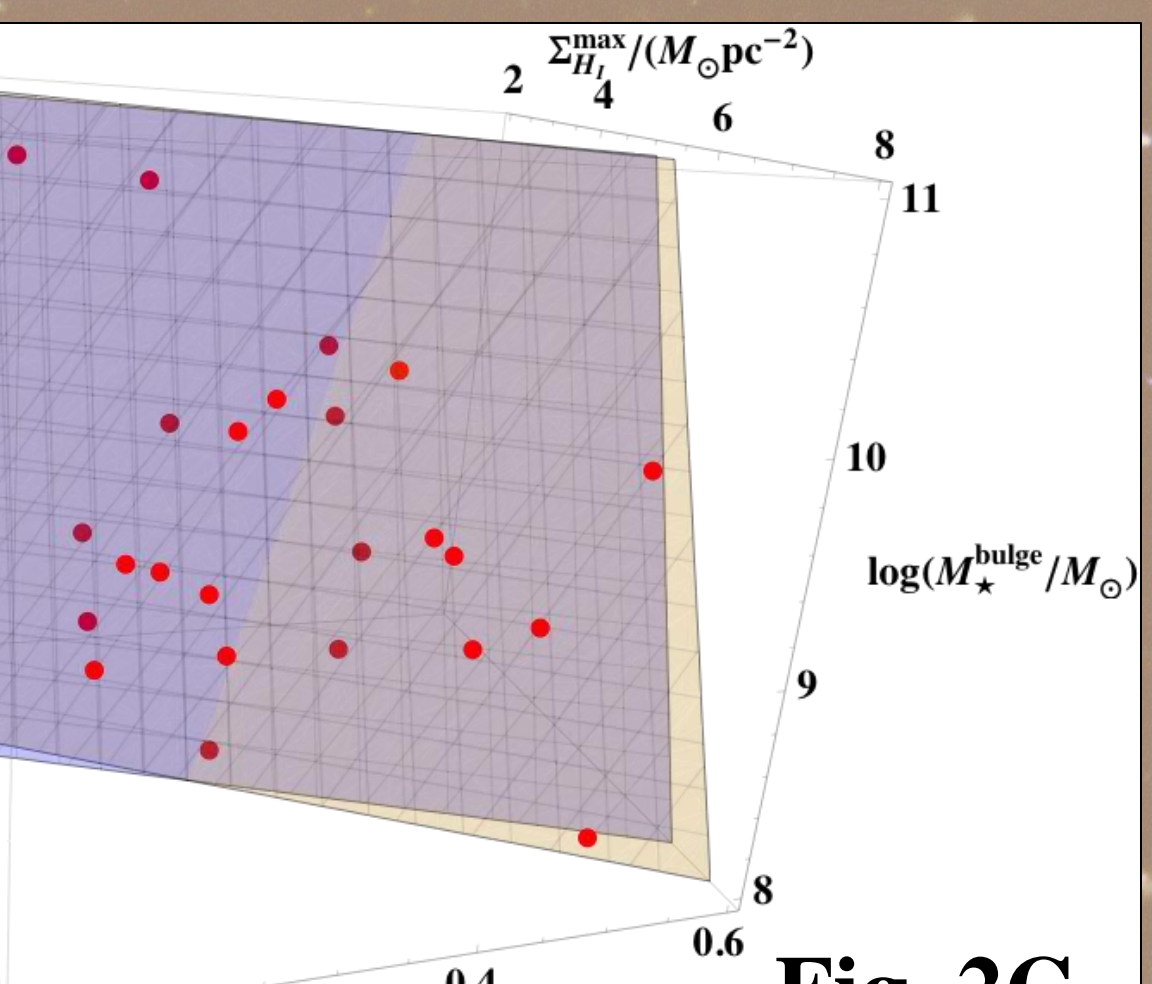


Fig. 2C

We find a best fit for Equation (1) from the included data sample of 24 galaxies (see Table 1) with a linear fit of

$$\tan|P| = (0.431 \pm 0.125) \frac{\sum_{H_I}^{\max} / (M_{\text{Sun}} \text{pc}^{-2})}{\log(M_{\text{stellar}}^{\text{bulge}} / M_{\text{Sun}})} + (0.098 \pm 0.071).$$

The residual standard error (intrinsic dispersion or scatter) is equal to 0.0945 (31.7 % per galaxy on average), with an adjusted $R^2 = 0.321$, and a p -value equal to 0.00232. A plot of this linear best fit is depicted along with the included data sample and can be seen in the above Figure 1 with the fit plotted as a dashed blue line. Alternatively, when taking into account the individual errors on measurements with a Monte Carlo sampling by creating multivariate normal distributions with the mean and variance of each variable for all 24 galaxies with 10^5 cases for each variable, we find

$$\tan|P| = (0.371 \pm 0.000) \frac{\sum_{H_I}^{\max} / (M_{\text{Sun}} \text{pc}^{-2})}{\log(M_{\text{stellar}}^{\text{bulge}} / M_{\text{Sun}})} + (0.130 \pm 0.000).$$

The residual standard error is equal to 0.114 (41.3 % per galaxy) and an adjusted $R^2 = 0.228$. This fit is plotted as a solid red line above.

The formula describing the fundamental plane for spiral galaxies from the included data sample of 24